

Control of tearing modes in toroidal fusion experiments using “designer” error fields

Richard Fitzpatrick and Enrico Rossi

Citation: *Physics of Plasmas* (1994-present) **8**, 2760 (2001); doi: 10.1063/1.1365956

View online: <http://dx.doi.org/10.1063/1.1365956>

View Table of Contents: <http://scitation.aip.org/content/aip/journal/pop/8/6?ver=pdfcov>

Published by the [AIP Publishing](#)

Articles you may be interested in

[Simulation and design of feedback control on resistive wall modes in Keda Torus eXperiment](#)

Phys. Plasmas **21**, 122506 (2014); 10.1063/1.4903529

[Neoclassical tearing modes and their control](#)

Phys. Plasmas **13**, 055501 (2006); 10.1063/1.2180747

[Modeling of neoclassical tearing mode stability for generalized toroidal geometry](#)

Phys. Plasmas **9**, 4567 (2002); 10.1063/1.1512285

[Control of neoclassical tearing modes in DIII-D](#)

Phys. Plasmas **9**, 2051 (2002); 10.1063/1.1456066

[Effect of rigid toroidal rotation on the stability of a tokamak plasma to tearing modes](#)

Phys. Plasmas **4**, 239 (1997); 10.1063/1.872137



PFEIFFER VACUUM

VACUUM SOLUTIONS FROM A SINGLE SOURCE

Pfeiffer Vacuum stands for innovative and custom vacuum solutions worldwide, technological perfection, competent advice and reliable service.

125 YEARS NOTHING IS BETTER

Control of tearing modes in toroidal fusion experiments using “designer” error fields

Richard Fitzpatrick and Enrico Rossi

Institute for Fusion Studies, Department of Physics, University of Texas at Austin, Austin, Texas 78712

(Received 17 October 2000; accepted 20 February 2001)

It is demonstrated that a magnetic island chain formed by a saturated tearing instability in a toroidal magnetic fusion device can lock to a special class of externally generated magnetic perturbation in a *stabilizing* phase. The theoretical apparatus needed to design such perturbations is outlined. These special perturbations—which are termed “designer” error fields—could be used to control the amplitudes of tearing modes in toroidal magnetic fusion experiments without the requirement of fast phase modulation. This type of control would be far more feasible in a reactor environment than conventional active feedback control via external magnetic perturbations. © 2001 American Institute of Physics. [DOI: 10.1063/1.1365956]

I. INTRODUCTION

Recent experimental results strongly suggest that further progress in obtaining thermonuclear reactor grade plasmas in either tokamaks or reversed-field pinches (RFPs) is dependent on the development of some reliable method for controlling the amplitudes of relatively low mode-number tearing modes, resonant within the plasma.^{1–5} Tearing modes are naturally unstable in toroidal magnetic fusion devices;⁶ they are driven by radial gradients in the plasma current density⁷ and plasma pressure,⁸ and generally saturate at relatively low amplitudes (i.e., $\tilde{B}/B \lesssim 1\%$).^{9–12} As the name suggests, “tearing modes” tear and reconnect magnetic field lines to produce helical chains of magnetic islands inside the plasma. Such island chains degrade plasma confinement because both heat and particles are able to travel radially from one side of an island chain to the other by flowing along magnetic field lines, which is a relatively fast process, instead of having to diffuse across magnetic flux surfaces, which is a relatively slow process.¹³

Currently, one of the most promising options for controlling tearing mode amplitudes in toroidal fusion devices is active feedback by means of externally applied, helical magnetic perturbations. Active control has already been implemented in a handful of tokamak experiments,^{14–16} with some degree of success. Unfortunately, it is highly doubtful whether an active magnetic feedback system would be feasible in a reactor environment. As is well known, a magnetic island chain naturally locks to a resonant magnetic perturbation in a helical phase such that the perturbation has a destabilizing effect on the chain. In fact, the stabilizing phase is *dynamically unstable*. The typical time scale for the development of the so-called *phase instability*,¹⁷ which causes an island chain in a stabilizing phase relation with a resonant perturbation to switch to a destabilizing relation, is only a few milliseconds. Thus, an active feedback system must be capable of modifying the phase of the applied magnetic perturbation on such a time scale in order to maintain a stabilizing phase relation. This inevitably implies that the coils that generate the feedback signals must be located *inside* any

of the conducting structures surrounding the plasma—otherwise, the signals would be shielded from the plasma by eddy currents. Unfortunately, placing feedback coils this close to a thermonuclear plasma is essentially impossible in a reactor environment—the necessary shielding to protect the coils from the neutron and heat flux emanating from the plasma, not to mention the mechanical support structure required to prevent the coils from being ripped off during a plasma disruption, would simply not fit in the available space.

Suppose, for the sake of argument, that it were possible to design an external magnetic perturbation with the singular property that a magnetic island chain would lock to it in a *stabilizing* phase. We could control the amplitude of the island chain, using such a perturbation, without the need for fast phase modulation, because there would be no need to overcome the phase instability. This type of magnetic feedback would be feasible in a reactor environment, since the coils needed to generate the perturbation could be placed *outside* the conducting structures surrounding the plasma, where they could be properly shielded. Our aim in this paper is to demonstrate that the novel scenario just outlined is actually a real possibility.

This paper is organized as follows. In Secs. II and III, we take the rigorous perturbation analysis of Thyagaraja (1981),¹¹ which describes the nonlinear saturation of an m,n magnetic island chain, and extend it slightly to deal with a general toroidal pinch equilibrium (rather than just a tokamak equilibrium), island evolution on a resistive time scale, and nonlinear coupling of the island chain to lm,ln magnetic perturbations (for $l > 1$). We note, in passing, that Norris (1989)¹⁸ has published a paper criticizing Thyagaraja’s approach. We fully concur with Thyagaraja’s rebuttal of these criticisms.¹⁹ In Sec. IV, we demonstrate that as a tearing mode gradually becomes more unstable, and its saturated amplitude consequently increases, its island flux surfaces undergo a sequence of nonlinear distortions in which they are skewed radially, and, to a lesser extent, elongated in the direction of increasing helical angle. Finally, in Sec. V, we

show that the nonlinear effects that are responsible for these distortions profoundly modify the island dynamics in the presence of a special class of externally generated magnetic perturbation. A perturbation of this class is made up predominantly of lm,ln (where $l>1$) helical magnetic fields, with a much smaller m,n component. It is possible to adjust the relative amplitudes and phases of these components in such a manner that an m,n island chain of sufficiently large amplitude will lock to the perturbation in a stabilizing phase. We call such a perturbation a “designer” error field. Here, we use the term “error field,” rather loosely, to refer to a static, externally generated, magnetic perturbation.

Incidentally, we note that Chu *et al.*²⁰ have previously published a paper investigating the effect of lm,ln external magnetic perturbations on the growth of an m,n magnetic island. Both the method adopted and the results obtained in the Chu paper differ substantially from those reported here.

II. PRELIMINARY ANALYSIS

A. Plasma equilibrium

Consider a large aspect ratio,²¹ zero- β ,²² plasma equilibrium whose unperturbed magnetic flux surfaces map out (almost) concentric circles in the poloidal plane. Such an equilibrium is well approximated as a periodic cylinder. Suppose that the minor radius of the plasma is a . Standard cylindrical polar coordinates (r, θ, z) are adopted. The system is assumed to be periodic in the z direction, with periodicity length $2\pi R_0$, where R_0 is the simulated plasma major radius. It is convenient to define a simulated toroidal angle $\phi = z/R_0$.

The equilibrium magnetic field is written $\mathbf{B} = [0, B_\theta(r), B_\phi(r)]$, where $\nabla \wedge \mathbf{B} = \sigma(r)\mathbf{B}$.

B. Newcomb’s equation

The magnetic perturbation associated with an m,n tearing mode (i.e., a mode with m periods in the poloidal direction, and n periods in the toroidal direction) can be written as

$$\mathbf{b}(\mathbf{r}, t) = \mathbf{b}^{m,n}(r, t)e^{i\zeta}, \tag{1}$$

where $\zeta = m\theta - n\phi$ is a helical angle. Of course, the physical perturbation is the real part of the above expression. In this paper, it is assumed that $m > 0$ and $n \neq 0$. The linearized magnetic flux function $\psi^{m,n}(r, t) \equiv -irb_r^{m,n}$ satisfies Newcomb’s equation,²³

$$\frac{d}{dr} \left(f \frac{d\psi^{m,n}}{dr} \right) - g\psi^{m,n} = 0, \tag{2}$$

where

$$f(r) = \frac{r}{m^2 + n^2 \epsilon^2}, \tag{3}$$

$$g(r) = \frac{1}{r} + \frac{r(n\epsilon B_\theta + mB_\phi)}{(m^2 + n^2 \epsilon^2)(mB_\theta - n\epsilon B_\phi)} \frac{d\sigma}{dr} + \frac{2mn\epsilon\sigma}{(m^2 + n^2 \epsilon^2)^2} - \frac{r\sigma^2}{m^2 + n^2 \epsilon^2}, \tag{4}$$

and $\epsilon = r/R_0$. As is well known, Eq. (2) is *singular* at the m/n rational surface, minor radius r_s , which satisfies $F(r_s) = 0$, where $F(r) \equiv mB_\theta(r) - n\epsilon(r)B_\phi(r)$. This singularity is resolved by the presence of a thin nonlinear/nonideal region (i.e., a magnetic island chain) centered on the rational surface.

C. Asymptotic behavior of $\psi^{m,n}$ in the vicinity of the rational surface

Let $x = (r - r_s)/r_s$. The most general solution of Eq. (2) in the vicinity of the rational surface that is consistent with the physical requirement that $b_r^{m,n}$ be continuous across the island region is written as

$$\psi^{m,n}(x) = \Psi^{m,n} \left(1 + (A^{m,n} - \lambda_0 - \lambda_1)x + \lambda_0 x \ln|x| + \frac{\lambda_0(\lambda_0 - \lambda_1)}{2} x^2 \ln|x| \right) + \Delta \Psi^{m,n} \frac{|x|}{2} + O(x^2), \tag{5}$$

where

$$\lambda_0 = \left(\frac{r^2 \sigma'}{r\sigma - 2mn\epsilon/(m^2 + n^2 \epsilon^2)} \right)_{r_s}, \tag{6}$$

$$\lambda_1 = \left(\frac{m^2 - n^2 \epsilon^2}{m^2 + n^2 \epsilon^2} \right)_{r_s}, \tag{7}$$

and $' \equiv d/dr$. Here, $\Psi^{m,n}$ represents the *reconnected magnetic flux* at the m,n rational surface, whereas $\Delta \Psi^{m,n}$ is a measure of the m,n helical current flowing in the vicinity of this surface. The quantity $A^{m,n}$ has no particular physical significance. Note that $\Psi^{m,n}$, $\Delta \Psi^{m,n}$, and $A^{m,n}$ are all complex quantities.

D. Island region

Let us assume the existence of an m,n helical quasiequilibrium in the immediate vicinity of the rational surface. This is equivalent to the assumption that all quantities in this region are functions of r, ζ , and t alone. The equations governing the quasiequilibrium are

$$\nabla \cdot \mathbf{B} = 0, \tag{8}$$

$$\nabla \cdot \mathbf{V} = 0, \tag{9}$$

$$\nabla \wedge \mathbf{B} = \mu_0 \mathbf{J}, \tag{10}$$

$$\mathbf{J} \wedge \mathbf{B} = \mathbf{0}, \tag{11}$$

$$\mathbf{E} + \mathbf{V} \wedge \mathbf{B} = \eta \mathbf{J}, \tag{12}$$

where $\mathbf{E}, \mathbf{B}, \mathbf{J}$, and \mathbf{V} are the electric field, magnetic field, current density, and plasma velocity, respectively, and η is the (constant) parallel electrical resistivity in the vicinity of the rational surface. Note that plasma inertia, viscosity, and pressure are all neglected in this calculation. Without loss of generality, we can write

$$\mathbf{B} = C\nabla\psi \wedge \hat{\mathbf{n}} + B_{\parallel}\hat{\mathbf{n}}, \tag{13}$$

$$\mathbf{V} = C\nabla\chi \wedge \hat{\mathbf{n}} + V_{\parallel}\hat{\mathbf{n}}, \tag{14}$$

where ψ , χ , B_{\parallel} , and V_{\parallel} are functions of r , ζ , and t only. Here, $C(r) = (m^2 + n^2\epsilon^2)^{-1/2}$, whereas $\hat{\mathbf{n}}(r) = C(0, n\epsilon, m)$. Note that $\mathbf{B} \cdot \nabla\psi = \mathbf{V} \cdot \nabla\chi = 0$, so ψ and χ are the *magnetic flux function* and *velocity streamfunction*, respectively. Incidentally, we are able to express the \mathbf{B} and \mathbf{V} fields in above forms because all of the Fourier harmonics included in our calculation share the same helicity: i.e., the same ratio of poloidal to toroidal mode numbers.

It is easily demonstrated that

$$E_{\parallel} = C \frac{\partial\psi}{\partial t}, \tag{15}$$

and

$$\begin{aligned} \mu_0 J_{\parallel} = & - \left(C \frac{\partial^2\psi}{\partial r^2} + \frac{C}{r} \frac{\partial\psi}{\partial r} + 2 \frac{\partial C}{\partial r} \frac{\partial\psi}{\partial r} + \frac{C^{-1}}{r^2} \frac{\partial^2\psi}{\partial \zeta^2} \right) \\ & + C^2 \frac{2mn\epsilon}{r} B_{\parallel}, \end{aligned} \tag{16}$$

where $E_{\parallel} = \hat{\mathbf{n}} \cdot \mathbf{E}$, and $J_{\parallel} = \hat{\mathbf{n}} \cdot \mathbf{J}$. It is also possible to show that

$$B_{\parallel} = CG(\psi), \tag{17}$$

$$\mu_0 J_{\parallel} = CH(\psi), \tag{18}$$

$$H = G \frac{dG}{d\psi}. \tag{19}$$

Now, we can write

$$\psi(r, \zeta, t) = \psi_0(r) + \sum_{l=1}^{\infty} \frac{\psi^{lm,ln}(r, t)}{l} e^{il\zeta}, \tag{20}$$

$$H(r, \zeta, t) = H_0(r) + \sum_{l=1}^{\infty} \frac{H_l(r, t)}{l} e^{il\zeta}, \tag{21}$$

where $\psi_0(r) = -\int_{r_s}^r F(r') dr'$ and $H_0(r) = \sigma(n\epsilon B_{\theta} + mB_{\phi})$. Taylor expansion of ψ_0 and H_0 about $r = r_s$ yields

$$\psi_0(x) = -r_s F^{(0)} \left(\frac{x^2}{2} + F^{(1)} \frac{x^3}{6} + O(x^4) \right), \tag{22}$$

$$H_0(x) = H^{(0)} [1 + H^{(1)}x + O(x^2)], \tag{23}$$

with

$$F^{(0)} = \left(\frac{B_{\theta}}{n\epsilon} [r\sigma(m^2 + n^2\epsilon^2) - 2mn\epsilon] \right)_{r_s}. \tag{24}$$

Finally, the scalar product of $\hat{\mathbf{n}}$ with the perturbed Ohm's law gives

$$-C \frac{\partial\delta\psi}{\partial t} + \hat{\mathbf{n}} \cdot (\mathbf{V} \wedge \mathbf{B}) = \frac{C\eta}{\mu_0} \delta H, \tag{25}$$

where $\delta\psi = \psi - \psi_0$ and $\delta H = H - H_0$.

The complete set of island equations [i.e., Eqs. (16), (19), and (25)] takes the form

$$\begin{aligned} & - \frac{\partial\delta\psi}{\partial t} + \frac{1}{r} \left(\frac{\partial\chi}{\partial r} \frac{\partial\psi}{\partial \zeta} - \frac{\partial\chi}{\partial \zeta} \frac{\partial\psi}{\partial r} \right) \\ & = \frac{\eta}{\mu_0} \{ H - H^{(0)} [1 + H^{(1)}x + O(x^2)] \}, \end{aligned} \tag{26}$$

$$\begin{aligned} H = & - \frac{\partial^2\psi}{\partial r^2} - \frac{1}{r} \frac{\partial\psi}{\partial r} + \frac{2n^2\epsilon^2}{r(m^2 + n^2\epsilon^2)} \frac{\partial\psi}{\partial r} - \frac{(m^2 + n^2\epsilon^2)}{r^2} \frac{\partial^2\psi}{\partial \zeta^2} \\ & + \frac{2mn\epsilon}{r(m^2 + n^2\epsilon^2)} G, \end{aligned} \tag{27}$$

$$H = G \frac{dG}{d\psi}. \tag{28}$$

E. Normalized boundary conditions

Let

$$\Psi_l = \Psi^{lm,ln}, \tag{29}$$

$$\Delta\Psi_l = \Delta\Psi^{lm,ln}, \tag{30}$$

$$A_l = A^{lm,ln} \Psi^{lm,ln}. \tag{31}$$

Our fundamental normalizations are

$$\hat{\psi}(X, \zeta) = \frac{\psi}{\Psi_1}, \tag{32}$$

$$X = \frac{x}{\mu^{1/2}}, \tag{33}$$

where $\Psi_1(t)$ is assumed to be *real*, and

$$\mu = \frac{\Psi_1}{r_s F^{(0)}} \ll 1 \tag{34}$$

is our expansion parameter. Let

$$\Psi_l = \mu^{1/2} \Psi_1 \hat{\Psi}_l, \quad \text{for } l > 1, \tag{35}$$

$$\Delta\Psi_l = \mu^{1/2} \ln \mu^{-1/2} \Psi_1 \Delta\hat{\Psi}_l, \quad \text{for } l > 0, \tag{36}$$

$$A_l = \mu^{1/2} \ln \mu^{-1/2} \Psi_1 \hat{A}_l, \quad \text{for } l > 1. \tag{37}$$

Here, $\hat{\Psi}_l$, $\Delta\hat{\Psi}_l$, and \hat{A}_l are all designed to be $O(1)$ quantities.

Equations (5), (20), and (22) yield the following expression for the normalized magnetic flux function at the boundary of the island region:

$$\begin{aligned} \hat{\psi}(X, \zeta) = & - \left\{ \left(\frac{X^2}{2} - \cos \zeta \right) + \mu^{1/2} \ln \mu^{-1/2} \lambda_0 X \cos \zeta + \mu^{1/2} \left[(\lambda_0 - \lambda_1 \lambda_2 + \lambda_2 - 1) \frac{X^3}{6} - \lambda_0 X \ln |X| \cos \zeta - (\tilde{A})_r X \cos \zeta \right. \right. \\ & + (\tilde{A})_i X \sin \zeta - \sum_{l=2}^{\infty} \frac{(\hat{\Psi}_l)_r}{l} \cos l \zeta + \sum_{l=2}^{\infty} \frac{(\hat{\Psi}_l)_i}{l} \sin l \zeta \left. \right] + \mu \ln \mu^{-1/2} \left(\lambda_0 (\lambda_0 - \lambda_1) \frac{X^2}{2} \cos \zeta - |X| \sum_{l=1}^{\infty} \frac{(\Delta \hat{\Psi}_l)_r}{2l} \cos l \zeta \right. \\ & + |X| \sum_{l=1}^{\infty} \frac{(\Delta \hat{\Psi}_l)_i}{2l} \sin l \zeta - X \sum_{l=2}^{\infty} \frac{(\hat{A}_l)_r}{l} \cos l \zeta + X \sum_{l=2}^{\infty} \frac{(\hat{A}_l)_i}{l} \sin l \zeta + \lambda_0 X \sum_{l=2}^{\infty} \frac{(\hat{\Psi}_l)_r}{l} \cos l \zeta - \lambda_0 X \sum_{l=2}^{\infty} \frac{(\hat{\Psi}_l)_i}{l} \sin l \zeta \left. \right) \\ & \left. + O(\mu) \right\}. \end{aligned} \tag{38}$$

Here, the subscripts r and i refer to real and imaginary parts, respectively. Moreover, $\tilde{A} = A^{m,n} - \lambda_0 - \lambda_1 \sim O(1)$, and

$$\lambda_2 = \left(\frac{r \sigma}{r \sigma - 2mn \epsilon / (m^2 + n^2 \epsilon^2)} \right)_{r_s}. \tag{39}$$

F. Normalized island equations

Let

$$\hat{J}(\hat{\psi}) = \frac{r_s^2 \mu H}{\Psi_1}, \tag{40}$$

$$\hat{\chi} = - \frac{\mu_0 \chi}{\eta}, \tag{41}$$

$$\hat{B}_{\parallel}(\hat{\psi}) = \frac{r_s \mu G}{\Psi_1}. \tag{42}$$

Equations (26)–(28) reduce to the following set of normalized island equations:

$$\begin{aligned} - \mu \ln \mu^{-1/2} \lambda_4 \delta \hat{\psi} - \mu^{1/2} \left(\frac{\partial \hat{\chi}}{\partial X} \frac{\partial \hat{\psi}}{\partial \zeta} - \frac{\partial \hat{\psi}}{\partial X} \frac{\partial \hat{\chi}}{\partial \zeta} \right) \\ = \hat{J} - (\lambda_2 + \mu^{1/2} \lambda_0 X) + O(\mu), \end{aligned} \tag{43}$$

$$\hat{J} = - \frac{\partial^2 \hat{\psi}}{\partial X^2} + \lambda_3 [1 - \mu^{1/2} (1 - \lambda_1) X] \hat{B}_{\parallel} - \mu^{1/2} \lambda_1 \frac{\partial \hat{\psi}}{\partial X} + O(\mu), \tag{44}$$

$$\mu \hat{J} = \hat{B}_{\parallel} \frac{d \hat{B}_{\parallel}}{d \hat{\psi}}, \tag{45}$$

where $\delta \hat{\psi} = \delta \psi / \Psi_1$, and

$$\lambda_3 = \left(\frac{2mn \epsilon}{m^2 + n^2 \epsilon^2} \right)_{r_s}, \tag{46}$$

with

$$\lambda_4 = \frac{2 \tau_R}{\mu^{1/2} \ln \mu^{-1/2}} \frac{d \mu^{1/2}}{dt}. \tag{47}$$

Here, $\tau_R = r_s^2 \mu_0 / \eta$ is the resistive evolution time scale in the vicinity of the rational surface. In accordance with Rutherford (1973)⁹ and Thyagaraja (1981),¹¹ we assume that $\lambda_4 \sim O(1)$.

III. ASYMPTOTIC MATCHING

A. Introduction

Our task, in this section, is to solve the island equations, (43)–(45), and asymptotically match this solution to the boundary condition (38). Let us, first of all, adopt the following expansions:

$$\begin{aligned} \hat{\psi} = \hat{\psi}_0 + \mu^{1/2} \ln \mu^{-1/2} \hat{\psi}_1 + \mu^{1/2} \hat{\psi}_2 + \mu \ln \mu^{-1/2} \hat{\psi}_3 \\ + O(\mu), \end{aligned} \tag{48}$$

$$\hat{J} = \hat{J}_0 + \mu^{1/2} \ln \mu^{-1/2} \hat{J}_1 + \mu^{1/2} \hat{J}_2 + \mu \ln \mu^{-1/2} \hat{J}_3 + O(\mu), \tag{49}$$

$$\hat{B}_{\parallel} = \hat{B}_{\parallel 0} + O(\mu). \tag{50}$$

Note that $\hat{B}_{\parallel 0} = (\lambda_2 - 1) / \lambda_3$. Incidentally, it is clear from Eq. (45) that $\hat{B}_{\parallel 1} = \hat{B}_{\parallel 2} = \hat{B}_{\parallel 3} = 0$. In the following, the terms on the right-hand side of Eq. (48) will be referred to as zeroth-order, first-order, second-order, and third-order terms, respectively. We shall develop our matched island solution order by order.

B. Zeroth-order matching

To zeroth-order, Eqs. (43) and (44) yield

$$\hat{J}_0 = \lambda_2 = - \frac{\partial^2 \hat{\psi}_0}{\partial X^2} + \lambda_3 \hat{B}_{\parallel 0}. \tag{51}$$

It follows that

$$\frac{\partial^2 \hat{\psi}_0}{\partial X^2} = -1. \tag{52}$$

Matching to Eq. (38) at $O(1)$ gives

$$\hat{\psi}_0 = - \left(\frac{X^2}{2} - \cos \zeta \right). \tag{53}$$

As is well known, the above flux function maps out a chain of magnetic islands, centered on the rational surface, of maximum radial width,

$$W = 4 \mu^{1/2} r_s. \tag{54}$$

The separatrix lies at $\hat{\psi}_0 = -1$. Moreover, the island O points and X points lie at $\zeta = j2\pi$ and $\zeta = (2j - 1)\pi$, respectively, where j is an integer. (See Fig. 1.) Note that

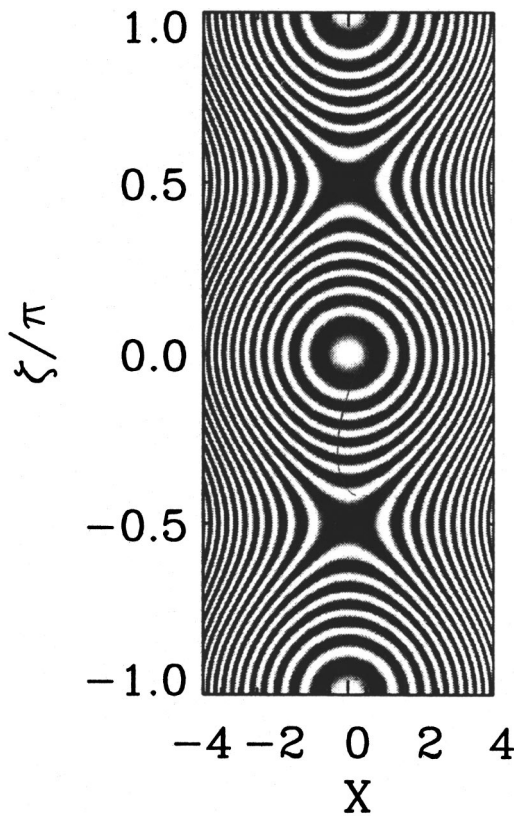


FIG. 1. Island flux surfaces calculated from Eq. (101), using the parameters listed in Table I. The stability index for the fundamental harmonic takes the value $E_1=0$.

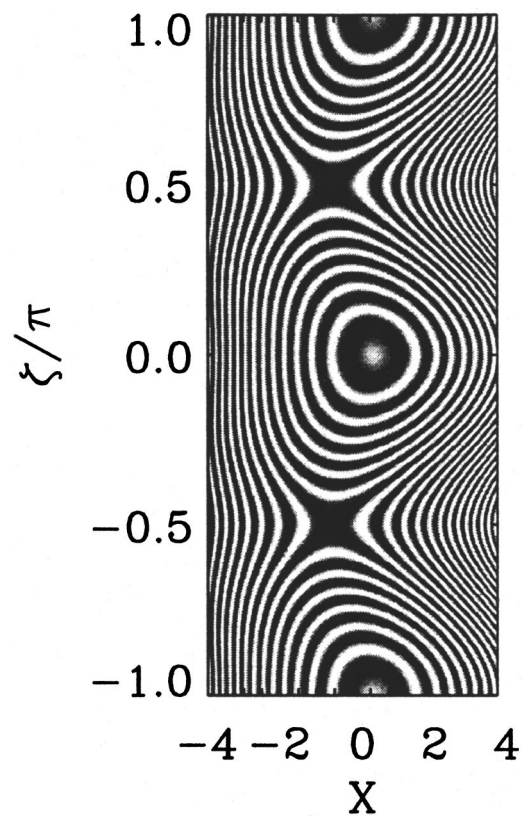


FIG. 2. Island flux surfaces calculated from Eq. (101), using the parameters listed in Table I. The stability index for the fundamental harmonic takes the value $E_1=5$.

$$\delta\hat{\psi}_0 = \cos \zeta. \tag{55}$$

C. First-order matching

To first order, Eqs. (43) and (44) yield

$$\hat{J}_1 = -\frac{\partial^2 \hat{\psi}_1}{\partial X^2} = 0. \tag{56}$$

Matching to Eq. (38) at $O(\mu^{1/2} \ln \mu^{-1/2})$ gives

$$\hat{\psi}_1 = -\lambda_0 X \cos \zeta. \tag{57}$$

This higher-order term gives rise to a slight distortion in the island structure, displacing the X points radially in one direction, and the O points in the opposite direction. (See Fig. 2.)

D. Flux-surface averaging

It is helpful to define a set of island coordinates:

$$s = \text{sgn}(X), \tag{58}$$

$$\Omega = -\hat{\psi}, \tag{59}$$

$$\zeta = m\theta - n\phi. \tag{60}$$

To lowest order, the island separatrix lies at $\Omega=1$. The flux-surface average operator $\langle \dots \rangle$ is defined as

$$\langle f(s, \Omega, \zeta) \rangle = \begin{cases} \oint \frac{f(s, \Omega, \zeta)}{|\partial \hat{\psi} / \partial X|_\zeta} \frac{d\zeta}{2\pi}, & \text{for } \Omega \geq 1, \\ \int_{-\zeta_0}^{\zeta_0} \frac{[f(s, \Omega, \zeta) + f(-s, \Omega, \zeta)]}{2|\partial \hat{\psi} / \partial X|_\zeta} \frac{d\zeta}{2\pi}, & \text{for } \Omega < 1, \end{cases} \tag{61}$$

where $X(s, \Omega, \zeta_0) = 0$. It is easily demonstrated that

$$\left\langle \frac{\partial \hat{\chi}}{\partial X} \frac{\partial \hat{\psi}}{\partial \zeta} - \frac{\partial \hat{\psi}}{\partial X} \frac{\partial \hat{\chi}}{\partial \zeta} \right\rangle = 0, \tag{62}$$

irrespective of the form of $\hat{\chi}$.

E. Higher-order matching

Flux-surface averaging of Eq. (43) yields

$$\hat{J}(\hat{\psi}) = \lambda_2 + \mu^{1/2} \lambda_0 \frac{\langle X \rangle}{\langle 1 \rangle} - \mu \ln \mu^{-1/2} \lambda_4 \frac{\langle \delta \hat{\psi} \rangle}{\langle 1 \rangle}. \tag{63}$$

Let

$$\hat{J}_{(2)} = \hat{J}_2 + \mu^{1/2} \ln \mu^{-1/2} \hat{J}_3. \tag{64}$$

It follows that

$$\hat{J}_{(2)} = \lambda_0 \frac{\langle X \rangle_{(1)}}{\langle 1 \rangle_{(1)}} - \mu^{1/2} \ln \mu^{-1/2} \lambda_4 \frac{\langle \cos \zeta \rangle_{(0)}}{\langle 1 \rangle_{(0)}}, \tag{65}$$

where the subscript (0)/(1) on a flux-surface average indicates that the average in question must be calculated with $\hat{\psi}$ evaluated to zeroth/first order.

As is easily demonstrated, to first order,

$$X = \sqrt{2(\Omega + \cos \zeta)} - \mu^{1/2} \ln \mu^{-1/2} \lambda_0 \cos \zeta, \quad (66)$$

$$\left| \frac{\partial \hat{\psi}}{\partial X} \right|_{\zeta} = \sqrt{2(\Omega + \cos \zeta)}. \quad (67)$$

It follows that

$$\hat{J}_{(2)} = \lambda_0 \frac{\langle X \rangle_{(0)}}{\langle 1 \rangle_{(0)}} - \mu^{1/2} \ln \mu^{-1/2} (\lambda_0^2 + \lambda_4) \frac{\langle \cos \zeta \rangle_{(0)}}{\langle 1 \rangle_{(0)}}. \quad (68)$$

F. Second-order matching

Equation (68) yields

$$\hat{J}_2 = \lambda_0 \frac{\langle X \rangle_{(0)}}{\langle 1 \rangle_{(0)}}. \quad (69)$$

At large $|X|$, this expression reduces to

$$\hat{J}_2 = \lambda_0 \left(X - \frac{\cos \zeta}{X} \right) + \mu^{1/2} \ln \mu^{-1/2} \lambda_0^2 \cos \zeta + O(\mu^{1/2}) + O\left(\frac{1}{X^2}\right). \quad (70)$$

The second term on the right-hand side should properly be included in the large $|X|$ expansion of \hat{J}_3 .

According to Eq. (44),

$$\begin{aligned} \hat{J}_2 &= -\frac{\partial^2 \hat{\psi}_2}{\partial X^2} - \lambda_3(1 - \lambda_1)XB_{10} - \lambda_1 \frac{\partial \hat{\psi}_0}{\partial X} \\ &= -\frac{\partial^2 \hat{\psi}_2}{\partial X^2} + [\lambda_1 \lambda_2 - \lambda_2 + 1]X. \end{aligned} \quad (71)$$

Hence, at large $|X|$,

$$\frac{\partial^2 \hat{\psi}_2}{\partial X^2} = -[\lambda_0 - \lambda_1 \lambda_2 + \lambda_2 - 1]X + \frac{\lambda_0 \cos \zeta}{X} + O\left(\frac{1}{X^2}\right). \quad (72)$$

Integrating, and matching to Eq. (38) at $O(\mu^{1/2})$, we obtain

$$\begin{aligned} \hat{\psi}_2 &= -[\lambda_0 - \lambda_1 \lambda_2 + \lambda_2 - 1] \frac{X^3}{6} + \lambda_0 X \ln |X| \cos \zeta \\ &\quad + (\tilde{A})_r X \cos \zeta - (\tilde{A})_i X \sin \zeta + \sum_{l=2}^{\infty} \frac{(\hat{\Psi}_l)_r}{l} \cos l\zeta \\ &\quad - \sum_{l=2}^{\infty} \frac{(\hat{\Psi}_l)_i}{l} \sin l\zeta. \end{aligned} \quad (73)$$

G. Third-order matching

Equation (68) yields

$$J_3 = -\lambda_5 \frac{\langle \cos \zeta \rangle_{(0)}}{\langle 1 \rangle_{(0)}}, \quad (74)$$

where $\lambda_5 = \lambda_0^2 + \lambda_4$. At large $|X|$, this expression reduces to

$$\hat{J}_3 \sim O\left(\frac{1}{X^2}\right). \quad (75)$$

According to Eq. (44),

$$\hat{J}_3 + \lambda_0^2 \cos \zeta = -\frac{\partial^2 \hat{\psi}_3}{\partial X^2} - \lambda_1 \frac{\partial \hat{\psi}_1}{\partial X}. \quad (76)$$

Here, we have included the $(\mu^{1/2} \ln \mu^{-1/2})$ contribution from the large $|X|$ expansion of \hat{J}_2 . Hence,

$$\frac{\partial^2 \hat{\psi}_3}{\partial X^2} = -\hat{J}_3 - \lambda_0(\lambda_0 - \lambda_1) \cos \zeta. \quad (77)$$

Let

$$\begin{aligned} \hat{\psi}_{3'} &= \hat{\psi}_3 + \lambda_0(\lambda_0 - \lambda_1) \frac{X^2}{2} \cos \zeta - X \sum_{l=2}^{\infty} \frac{(\hat{A}_l)_r}{l} \cos l\zeta \\ &\quad + X \sum_{l=2}^{\infty} \frac{(\hat{A}_l)_i}{l} \sin l\zeta + \lambda_0 X \sum_{l=2}^{\infty} \frac{(\hat{\Psi}_l)_r}{l} \cos l\zeta \\ &\quad - \lambda_0 X \sum_{l=2}^{\infty} \frac{(\hat{\Psi}_l)_i}{l} \sin l\zeta. \end{aligned} \quad (78)$$

It follows that

$$\frac{\partial^2 \hat{\psi}_{3'}}{\partial X^2} = -\hat{J}_3. \quad (79)$$

According to Eq. (38), at large $|X|$,

$$\hat{\psi}_{3'} = |X| \sum_{l=1}^{\infty} \frac{(\Delta \hat{\Psi}_l)_r}{2l} \cos l\zeta - |X| \sum_{l=1}^{\infty} \frac{(\Delta \hat{\Psi}_l)_i}{2l} \sin l\zeta. \quad (80)$$

At this stage, we have matched all terms in Eq. (38), except for those involving $\Delta \hat{\Psi}_l$.

H. Evaluation of Λ_l

It is clear from Eq. (74) that $\hat{J}_3 = \hat{J}_3(X, \cos \zeta)$. Hence, it follows from symmetry, and Eq. (80), that

$$(\Delta \hat{\Psi}_l)_i = 0, \quad (81)$$

for all $l > 0$. In other words, the $\Delta \hat{\Psi}_l$ are real quantities. Let

$$\Delta \hat{\Psi}_l = l \Lambda_l \lambda_5, \quad (82)$$

for all $l > 0$. Furthermore, let

$$\frac{\hat{J}_3}{\lambda_5} = \frac{\tilde{J}_0(X)}{2} + \sum_{l=1}^{\infty} \tilde{J}_l(X) \cos l\zeta, \quad (83)$$

$$\frac{\hat{\psi}_{3'}}{\lambda_5} = \frac{P_0(X)}{2} + \sum_{l=1}^{\infty} P_l(X) \cos l\zeta. \quad (84)$$

It follows from Eq. (79) that

$$\frac{d^2 P_l}{dX^2} = -\tilde{J}_l, \quad (85)$$

for $l = 0, \dots, \infty$. Hence,

$$\frac{dP_l}{dX} \Big|_{X \rightarrow \infty} - \frac{dP_l}{dX} \Big|_{X \rightarrow -\infty} = -2 \int_0^{\infty} \tilde{J}_l(X) dX = \Lambda_l. \quad (86)$$

TABLE I. Data calculated for an $m=2, n=1$ tearing mode in a large aspect ratio (i.e., $\epsilon_s \rightarrow 0$), zero- β tokamak equilibrium characterized by $\sigma = \sigma_0 [1 - (r/a)^2]^{2.768}$. The values of the safety factor at the center and edge of the plasma are $q_0=0.85$ and $q_a=3.2$, respectively. Also, $r_s=0.7787a$, $c=1.15a$, and $\lambda_0=-8.515$.

l	Poloidal mode number	Toroidal mode number	Λ_l	E_l	\mathcal{A}_l
0	+0.0000
1	2	1	+1.6454	+2.826	1.964
2	4	2	+1.7058e-1	-5.148	1.502
3	6	3	-3.3174e-2	-10.06	1.009
4	8	4	+1.2816e-2	-14.52	0.6193
5	10	5	-6.4520e-3	-18.81	0.3580
6	12	6	+3.7622e-3	-23.00	0.1987
7	14	7	-2.4113e-3	-27.15	0.1071
8	16	8	+1.6539e-3	-31.25	5.646e-2

Here, we have made use of the fact that \hat{J}_3 is an even function of X . Note that we require $\Lambda_0=0$ for self-consistent matching. It follows that

$$\Lambda_l = -2 \int_0^\infty \tilde{J}_l(X) dX = -\frac{2}{\pi} \int_0^\infty \int_{-\pi}^\pi \frac{\hat{J}_3(\Omega)}{\lambda_5} \cos l\zeta d\zeta dX. \quad (87)$$

Finally, changing to island coordinates, we obtain

$$\Lambda_l = 4 \int_{-1}^\infty \frac{\langle \cos \zeta \rangle_{(0)} \langle \cos l\zeta \rangle_{(0)}}{\langle 1 \rangle_{(0)}} d\Omega. \quad (88)$$

Computation of the above integral gives the Λ_l values listed in Table I. Note that $\Lambda_0=0$, in accordance with our earlier requirement.

I. Evaluation of $\Delta\Psi_l$

Equations (36), (47), (54), and (82) yield

$$\Delta\Psi_l = l\Lambda_l\Psi_1 \left[\lambda_0^2 \left(\frac{W}{4r_s} \right) \ln \left(\frac{4r_s}{W} \right) + \frac{\tau_R}{2} \frac{d(W/r_s)}{dt} \right], \quad (89)$$

for $l>0$, assuming that Ψ_1 is real. Let us now relax this restriction. Suppose that

$$\Psi_1 = \hat{\Psi}_1 e^{-i\varphi_1}, \quad (90)$$

where $\hat{\Psi}_1$ and φ_1 are both real. As is easily demonstrated, the generalization of Eq. (89) is

$$\Delta\Psi_l = l\Lambda_l \hat{\Psi}_1 e^{-il\varphi_1} \left[\lambda_0^2 \left(\frac{W}{4r_s} \right) \ln \left(\frac{4r_s}{W} \right) + \frac{\tau_R}{2} \frac{d(W/r_s)}{dt} \right], \quad (91)$$

for $l>0$. For the case $l=1$, the above formula is similar to that obtained previously by Thyagaraja.¹¹ However, the extension of this formula to cover $l>1$ is a new result.

IV. NONLINEAR ISLAND COUPLING

A. Introduction

Our aim in this section is to investigate the growth and saturation of an n, m tearing mode in light of Eq. (91). In particular, we shall be interested in quantifying the coupling of the m, n harmonic—which we shall refer to as the *fundamental*, or $l=1$, harmonic—to the various lm, ln harmonics (where $l>1$)—which we shall refer to as *overtone*, or $l>1$, harmonics—via nonlinear effects in the island region.

mental, or $l=1$, harmonic—to the various lm, ln harmonics (where $l>1$)—which we shall refer to as *overtone*, or $l>1$, harmonics—via nonlinear effects in the island region.

B. Perturbed magnetic field

The perturbed magnetic field in the *outer region* (i.e., everywhere apart from the island region) can be written as

$$\delta\mathbf{B} = C\nabla\delta\psi \wedge \hat{\mathbf{n}}, \quad (92)$$

where

$$\delta\psi(r, \theta, \phi, t) = \sum_{l=1}^{\infty} \frac{\Psi_l(t) \hat{\psi}^{lm, ln}(r)}{l} e^{il\zeta}. \quad (93)$$

Here, $\hat{\psi}^{lm, ln}(r)$ represents the normalized lm, ln tearing eigenfunction. In other words, $\hat{\psi}^{lm, ln}(r)$ is a *real*, continuous solution to Newcomb's equation (2), which is well behaved as $r \rightarrow 0$, and satisfies $\hat{\psi}^{lm, ln}(r_s) = 1$ and $\hat{\psi}^{lm, ln}(c) = 0$. Here, we have assumed the presence of a conducting shell located, outside the plasma, at minor radius $r=c$. This prescription uniquely specifies $\hat{\psi}^{lm, ln}(r)$. In general, $\hat{\psi}^{lm, ln}(r)$ possesses a gradient discontinuity at $r=r_s$. The real quantity,

$$E_l = \left(r \frac{d\hat{\psi}^{lm, ln}(r)}{dr} \right)_{r_s-}^{r_s+} \quad (94)$$

can be identified as the standard *linear stability index*⁶ for the lm, ln tearing mode. In this paper, it is assumed that $E_1 > 0$ and $E_l < 0$ (for $l > 1$). In other words, the fundamental harmonic is linearly unstable, whereas the overtone harmonics are linearly stable.

C. Asymptotic matching

Equation (91) encapsulates the nonlinear physics in the *inner region*: i.e., the island region. Standard asymptotic matching between the inner and outer regions yields⁶

$$\Delta\Psi_l = E_l\Psi_l, \quad (95)$$

for all $l > 0$.

For the fundamental harmonic, $l=1$, Eqs. (91) and (95) reduce to the well-known *Rutherford island evolution equation*,⁹

$$\frac{\Lambda_1}{2} \tau_R \frac{d(W/r_s)}{dt} = E_1 - \lambda_0^2 \Lambda_1 \left(\frac{W}{4r_s} \right) \ln \left(\frac{4r_s}{W} \right). \quad (96)$$

The second term on the right-hand side of the above formula is a nonlinear saturation term similar in form to that first obtained heuristically by White *et al.* (1977)¹⁰ and rigorously by Thyagaraja (1981).¹¹

According to Eq. (96), a linearly unstable m, n tearing mode for which

$$0 < E_1 < \frac{\lambda_0^2 \Lambda_1}{e}, \quad (97)$$

grows algebraically on a *resistive* time scale, and eventually *saturates* at an island width W_0 , satisfying

$$\left(\frac{W_0}{4r_s}\right) \ln\left(\frac{4r_s}{W_0}\right) = \frac{E_1}{\lambda_0^2 \Lambda_1}. \tag{98}$$

Of course, we require $W_0 \ll r_s$ in order for the ‘‘thin island’’ ordering adopted in the earlier part of this paper (i.e., $\mu \ll 1$) to remain valid.

For the overtone harmonics, $l > 1$, Eqs. (91) and (95) reduce to

$$\frac{\Psi_l}{\hat{\Psi}_1} = -\frac{lE_1}{(-E_l)} \frac{\Lambda_l}{\Lambda_1} e^{-il\varphi_1}, \tag{99}$$

where $\hat{\Psi}_1$ and φ_1 are defined in Eq. (90). The above expression specifies the amplitude and phase of the overtone harmonics generated, from the fundamental harmonic, via nonlinear coupling in the island region. In general, the amplitudes of the $l > 1$ harmonics are significantly smaller than that of the $l = 1$ harmonic, since $lE_1 \Lambda_l \ll (-E_l) \Lambda_1$ (for $l > 1$). It follows, from Eq. (93), that the perturbed magnetic field in the outer region consists of an $l = 1$ field, plus a relatively small admixture of $l > 1$ fields.

D. Island flux surfaces

The magnetic flux function in the island region is written [see Eq. (20)] as

$$\psi = \psi_0 + \delta\psi. \tag{100}$$

Let $\hat{\psi} = \psi/\hat{\Psi}_1$. It follows that for a *saturated* island chain,

$$\hat{\psi}(X, \zeta') = -\left(\frac{X^2}{2} - \cos \zeta'\right) - \frac{E_1}{\lambda_0 \Lambda_1} X \cos \zeta' - \sum_{l=2}^{\infty} \frac{E_l}{(-E_l)} \frac{\Lambda_l}{\Lambda_1} \cos l\zeta', \tag{101}$$

where $\zeta' = \zeta - \varphi_1$. Note that the second term on the right-hand side of the above expression corresponds to the $\hat{\psi}_1$ correction calculated in Sec. III C.

It can be seen that the island flux function $\hat{\psi}(X, \zeta)$, defined in Eq. (101), is parametrized by E_1 —the linear stability index of the fundamental harmonic. For a weakly unstable tearing mode that saturates at a relatively low amplitude, E_1 is small, and the nonlinear corrections to $\hat{\psi}$ [i.e., the second and third terms on the right-hand side of Eq. (101)] are unimportant. However, as the mode becomes more unstable and, consequently, saturates at a higher amplitude, E_1 increases, and the nonlinear corrections to $\hat{\psi}$ become more significant.

As an illustration of the effect of these nonlinear corrections, let us consider a saturated $m = 2, n = 1$ tearing mode in a large aspect ratio (i.e., $\epsilon_s \rightarrow 0$), zero- β tokamak equilibrium characterized by $\sigma(r) = \sigma_0[1 - (r/a)^2]^{2.765}$. The values of the ‘‘safety factor’’ at the center and edge of this equilibrium are $q_0 = 0.85$ and $q_a = 3.2$, respectively. Furthermore, the radius of the 2, 1 rational surface is $r_s = 0.7787a$, the radius of the conducting shell is $c = 1.15a$, and the saturation parameter λ_0 takes the value -8.515 . The values of the linear stability indices, E_l , for the fundamental and overtone harmonics are listed in Table I. Note, that $E_1 > 0$ and $E_l < 0$ (for

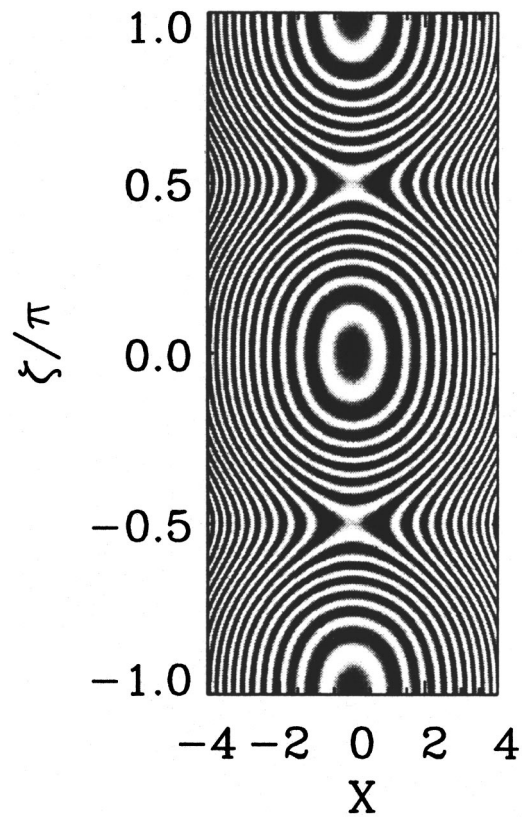


FIG. 3. Island flux surfaces calculated from Eq. (101), using the parameters listed in Table I. The ‘‘skew’’ term has been neglected. The stability index for the fundamental harmonic takes the value $E_1 = 10$.

$l > 1$), as previously assumed. In the following, we shall treat E_1 as a *variable* parameter, while assuming that all of the other parameters listed in Table I remain fixed. This treatment is justified, to some extent, because E_1 is far more sensitive to slight local (to the rational surface) changes in the current profile than any of the other parameters. For instance, we note that the overtone harmonic stability indices, E_l (for $l > 1$), listed in Table I, lie fairly close to their vacuum values, $-2lm$ (i.e., the values obtained by completely neglecting the effect of the plasma current).

Figure 1 shows island flux surfaces calculated using formula (101), and the parameters listed in Table I, for a low-amplitude, saturated tearing mode characterized by $E_1 = 0$. In this case, the nonlinear corrections are negligible, and the flux surfaces map out a conventional chain of symmetric magnetic islands. Figure 2 shows the corresponding flux surfaces for a higher-amplitude tearing mode characterized by $E_1 = 5$. It can be seen that the nonlinear corrections have the effect of radially *skewing* the island chain, such that it is flattened on the inner side of the rational surface, and distended on the outer side. This ‘‘skew’’ in the island structure is generated by the ‘‘current gradient’’ term (i.e., the second term on the right-hand side) in Eq. (101). In order to visualize the much smaller distortions in island structure generated by the overtone harmonic term (i.e., the third term on the right-hand side) in Eq. (101), we have suppressed the ‘‘skew’’ term in Fig. 3, and increased E_1 to 10. It can be seen that the overtone harmonic distortion acts to *elongate*

the island flux surfaces along the direction of $\nabla\zeta$.

We conclude that as a tearing mode gradually becomes more unstable, and its saturated amplitude consequently increases, its island flux surfaces undergo a sequence of nonlinear distortions in which they are skewed radially, and, to a lesser extent, elongated in the direction of an increasing helical angle. As we shall see, the nonlinear effects that are responsible for these distortions can profoundly modify the island dynamics in the presence of a particular class of externally generated magnetic perturbation.

V. MULTIHARMONIC ERROR FIELDS

A. Introduction

In the previous section, we demonstrated that a saturated m, n tearing mode is weakly coupled to overtone magnetic perturbations—i.e., perturbations whose mode numbers are lm, ln (for $l > 1$)—via nonlinear physics in the island region. It seems plausible, therefore, that such a mode should respond—albeit, weakly—to an externally generated $l > 1$ magnetic perturbation—i.e., an $l > 1$ “error field.” Obviously, an m, n mode will also respond strongly to an $l = 1$ error field. Let us investigate the dynamics of an m, n magnetic island chain in the presence of a stationary error field that is a superposition of $l = 1$ and $l > 1$ magnetic perturbations.

B. Error-field characteristics

Suppose that, in the absence of plasma, the error-field takes the form

$$\delta\mathbf{B}_{\text{vac}} = C\nabla\delta\psi_{\text{vac}}\wedge\hat{\mathbf{n}}. \quad (102)$$

Let

$$\Phi_l = \oint \oint l\delta\psi_{\text{vac}}(c, \theta, \phi)e^{-il(m\theta - n\phi)} \frac{d\theta}{2\pi} \frac{d\phi}{2\pi} \quad (103)$$

be (l times) the lm, ln Fourier harmonic of the error-field flux function, $\delta\psi_{\text{vac}}$, evaluated just inside the conducting shell (i.e., at $r = c$). It is simplest to imagine that the error field is either generated externally, and filters through thin gaps in the shell, or is produced via a helical displacement of the shell. We can write

$$\Phi_l = \hat{\Phi}_l e^{-i\alpha_l}, \quad (104)$$

where $\hat{\Phi}_l$ and α_l are both real.

C. Asymptotic matching

In the presence of the error-field, standard asymptotic matching yields²⁴

$$\Delta\Psi_l = E_l\Psi_l + \mathcal{A}_l\hat{\Phi}_l, \quad (105)$$

for $l > 0$, where

$$\mathcal{A}_l = \frac{i\hat{\psi}^{l, lm}(a)l^2(m^2 + n^2\epsilon_s^2)}{k_{lm}(ln\epsilon_c)i_{lm}(ln\epsilon_a) - k_{lm}(ln\epsilon_a)i_{lm}(ln\epsilon_c)}. \quad (106)$$

Here,

$$i_m(n\epsilon) = |n\epsilon|I_{m+1}(|n\epsilon|) + mI_m(|n\epsilon|), \quad (107)$$

$$k_m(n\epsilon) = -|n\epsilon|K_{m+1}(|n\epsilon|) + mK_m(|n\epsilon|), \quad (108)$$

where I_m and K_m represent standard modified Bessel functions. Furthermore, $\epsilon_a = a/R_0$ and $\epsilon_c = c/R_0$.

For $l = 1$, Eqs. (91) and (105) can be combined to give the error-field modified Rutherford island evolution equation:

$$\frac{\Lambda_1}{2} \tau_R \frac{d(W/r_s)}{dt} = E_1 - \lambda_0^2 \Lambda_1 \left(\frac{W}{4r_s} \right) \ln \left(\frac{4r_s}{W} \right) + \frac{\mathcal{A}_1 \hat{\Phi}_1}{\hat{\Psi}_1} \cos \varphi, \quad (109)$$

where $\varphi = \varphi_1 - \alpha_1$ is the island phase relative to that of the $l = 1$ error field. Note that, to lowest order, only the $l = 1$ component of the error field has any influence on the island width.

Now, the net toroidal electromagnetic torque exerted on the island region by the error field takes the form²⁴

$$\delta T_{\phi \text{ EM}} = \frac{2\pi^2 R_0}{\mu_0} \frac{n}{m^2 + n^2\epsilon_s^2} \sum_{l=1}^{\infty} \text{Im} \left\{ \frac{\Delta\Psi_l \Psi_l^*}{l} \right\}. \quad (110)$$

Equations (91), (105), and (109) can be combined with the above expression to give

$$\delta T_{\phi \text{ EM}} = \frac{2\pi^2 R_0}{\mu_0} \frac{n}{m^2 + n^2\epsilon_s^2} \mathcal{A}_1 \hat{\Phi}_1 \hat{\Psi}_1 \left\{ \sin \varphi - \sum_{l=2}^{\infty} \frac{\mathcal{A}_l \hat{\Phi}_l}{\mathcal{A}_1 \hat{\Phi}_1} \frac{\tilde{E}_1}{(-E_l)} \frac{\Lambda_l}{\Lambda_1} \sin(l\varphi - \delta_l) \right\}, \quad (111)$$

where $\delta_l = \alpha_l - l\alpha_1$, and

$$\tilde{E}_1 = E_1 + \frac{\mathcal{A}_1 \hat{\Phi}_1}{\hat{\Psi}_1} \cos \varphi. \quad (112)$$

Note that the $l > 1$ components of the error field contribute to the torque.

According to the above analysis, the $l > 1$ components of the external error field are able to penetrate freely into the island region, and beyond (i.e., into the plasma core). The reason for this is that the presence of $l > 1$ flux in the island region gives rise to a shape distortion of the island flux surfaces, but does not drive magnetic reconnection (see Sec. IV). Of course, flux surface shape distortions take place on the (effectively instantaneous) hydromagnetic time scale, whereas reconnection proceeds on a much slower time scale. Note, however, that this result is strongly dependent on the orderings made in Sec. II. In particular, on the assumption that the amount of $l > 1$ flux in the island region is *small* compared to the amount of $l = 1$ flux [see Eq. (35)].

D. Island dynamics

Since we are neglecting both plasma flow and viscosity in this paper, we expect the island chain to simply lock to the error field in a *stable* phase characterized by $\delta T_{\phi \text{ EM}} = 0$. The simplest method of distinguishing stable and unstable phases is to write an island equation of motion that incorporates phenomenological inertia and damping terms. For instance,²⁵

$$\iota \frac{d^2\varphi}{dt^2} + \nu \frac{d\varphi}{dt} + \left(\sin\varphi + E_1 \sum_{l=2}^{\infty} l a_l \sin(l\varphi - \delta_l) \right) = 0. \tag{113}$$

Here, ι and ν are positive constants, and the term in large parentheses represents the normalized toroidal electromagnetic torque. Incidentally, we are assuming that the second term on the right-hand side of Eq. (112) is small, for the sake of simplicity, so that we can make the approximation $\tilde{E}_1 \approx E_1$. It is helpful to associate a *locking potential* with the normalized torque. This is achieved by writing the above equation in the form

$$\iota \frac{d^2\varphi}{dt^2} + \nu \frac{d\varphi}{dt} + \frac{dV_{\text{lock}}}{d\varphi} = 0. \tag{114}$$

The potential $V_{\text{lock}}(\varphi)$ is given by

$$V_{\text{lock}}(\varphi) = -\cos\varphi - E_1 \sum_{l=2}^{\infty} a_l \cos(l\varphi - \delta_l). \tag{115}$$

The island dynamics is now trivial: the island chain locks to the error field at a phase that corresponds to a local *minimum* of the above potential. Note that as the chain becomes intrinsically more unstable (i.e., as E_1 gets bigger), and, therefore, grows to a larger saturated amplitude, the contribution of the $l > 1$ harmonics of the error field to the locking potential increases.

It is fairly straightforward to reconstruct the error field that generates the locking potential specified in Eq. (115). For instance, the normalized radial error field (in vacuum) just inside the shell takes the form

$$\delta \hat{B}_{r, \text{vac}}(\varphi_0) = \sin\varphi_0 - \sum_{l=2}^{\infty} a_l l (-E_l) \frac{\mathcal{A}_l \Lambda_1}{\mathcal{A}_l \Lambda_l} \sin(l\varphi_0 - \delta_l), \tag{116}$$

where $\varphi_0 = \zeta - \alpha_1$. Here, the field is conveniently normalized such that its $l = 1$ component has amplitude unity.

E. Example calculation

Consider an $m = 2, n = 1$ tearing mode in a large aspect ratio (i.e., $\epsilon_s \rightarrow 0$), zero- β tokamak equilibrium that is characterized by $\sigma(r) = \sigma_0 [1 - (r/a)^2]^{2.765}$, $q_0 = 0.85$, and $q_a = 3.2$. The Λ_l, E_l , and \mathcal{A}_l values for such a mode are listed in Table I. Let us investigate the dynamics of the associated 2,1 saturated magnetic island chain moving in the following locking potential:

$$V_{\text{lock}}(\varphi) = -\cos\varphi - E_1 (-1.4612 \cos 2\varphi + 0.5 \cos 3\varphi). \tag{117}$$

Note that this potential is generated from an error field that contains just *three* helical harmonics: namely, $l = 1, 2$, and 3 . Figure 4 plots the above potential for the case of a small-, medium-, and large-amplitude island chain—i.e., for $E_1 = 0, E_1 = 1$, and $E_1 = 3$, respectively.

For the small-amplitude case, $E_1 = 0$, the $l > 1$ harmonics of the error field make no contribution to the locking potential, which is consequently a pure sinusoid with a minimum at $\varphi = 0$. Hence, we expect the island chain to lock at $\varphi = 0$. Note, from Eq. (109), that the error field has a destabilizing

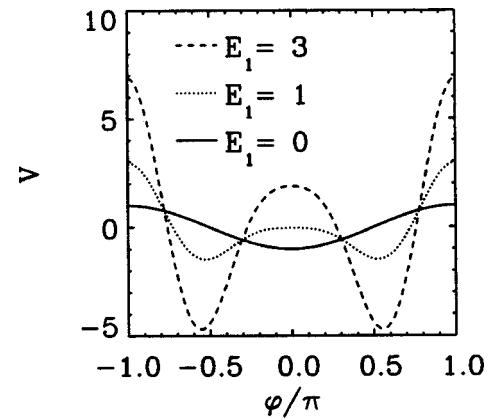


FIG. 4. The locking potential, $V_{\text{lock}}(\varphi)$, calculated from Eq. (117) for $E_1 = 0, 1$, and 3 .

effect on the chain whenever $-\pi/2 < \varphi < \pi/2$, and a stabilizing effect otherwise. It is clear, therefore, that the island chain locks to the error field in the *most destabilizing phase*. Of course, this is a well-known result.

For the medium amplitude case, $E_1 = 1$, nonlinear coupling in the island region allows the $l > 1$ harmonics of the error field to contribute to the locking potential. The modification of the potential is profound. The low-amplitude locking point, $\varphi = 0$, becomes unstable (i.e., $\varphi = 0$ is now a maximum, rather than a minimum, of the potential), and there are two new locking points located in the *stabilizing region*, i.e., $|\varphi| > \pi/2$. For the large-amplitude case, $E_1 = 3$, the situation is, more or less, the same, except that the locking points have rotated even farther into the stabilizing region.

We conclude that the locking potential (117) has a number of remarkable properties. At low amplitude, a resonant island chain locks to this potential in the most *destabilizing phase*—which is the conventional result. However, as the chain grows to larger amplitude, the potential is modified by nonlinear effects in such a manner that the locking point (i.e., the minimum of the potential) gradually rotates, until it is located in a *stabilizing phase*. Of course, the parameters in Eq. (117) have been carefully chosen to produce just such an effect.

Figure 5 shows the normalized, radial, vacuum magnetic

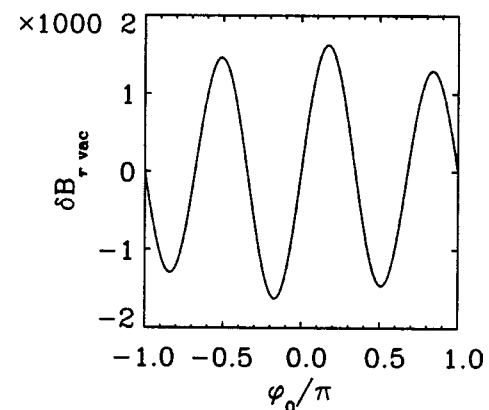


FIG. 5. The normalized, radial, vacuum magnetic perturbation, calculated at $r = c$, which generates the locking potential (117).

perturbation, calculated just inside the shell, which generates the locking potential (117). This perturbation can be written as

$$\delta \hat{B}_{r \text{ vac}}(\varphi_0) = \sin \varphi_0 + 189.75 \sin 2 \varphi_0 + 1456.8 \sin 3 \varphi_0. \quad (118)$$

It can be seen that the perturbation consists predominantly of an $l=3$ field, with a small $l=2$ component. Moreover, the $l=1$ component, whose amplitude is normalized to unity, is very much smaller in size than the other components. The reason that the $l>1$ components of the perturbation are much larger than the $l=1$ component is partly because $l>1$ fields decay more rapidly into the plasma than an $l=1$ field, and partly because the nonlinear coupling of $l=1$ and $l>1$ harmonics in the island region is comparatively weak. It should be noted that the 2, 1 tearing mode specified in Table I is not particularly unstable: $E_1=2.826$ corresponds to a saturated island width of $W/r_s \sim 0.5\%$. For a more unstable mode—destabilized, for instance, by the perturbed bootstrap current⁸—which attains a saturated amplitude of $W/r_s \sim 5\%$, we could reduce the amplitudes of the $l=2$ and $l=3$ components in Eq. (118) by an order of magnitude, and the error field would still generate the locking potentials shown in Fig. 4.

The magnetic perturbation shown in Fig. 5 is an example of what we term a “designer” error field. The relative amplitudes and phases of the helical components of this field have been carefully chosen such that a resonant magnetic island chain will lock to the field in a *stabilizing phase* when the chain grows to a sufficiently large amplitude. As discussed in the Introduction, it would be feasible to use such error fields to *control* the growth of tearing modes in tokamak or RFP reactors.

VI. SUMMARY

We have demonstrated, for the first time, the possibility that a magnetic island chain in a toroidal magnetic fusion device could lock to a special class of external magnetic perturbation in a *stabilizing phase*. As we have pointed out, it would be feasible to employ such perturbations to control

tearing mode amplitudes in a reactor environment. Our analysis is, by no means, comprehensive. Undoubtedly, a lot more research will be needed in order to transform the ideas contained in this paper into reality. Nevertheless, our initial results are extremely exciting!

ACKNOWLEDGMENTS

This research was funded by the U.S. Department of Energy, under Contracts No. DE-FG05-96ER-54346 and No. DE-FG03-98ER-54504.

- ¹T. Taylor, E. J. Strait, L. L. Lao *et al.*, Phys. Plasmas **2**, 2390 (1995).
- ²T. Ivers, E. Eisner, A. Garafalo *et al.*, Phys. Plasmas **3**, 1926 (1996).
- ³O. Sauter, R. J. LaHaye, Z. Chang *et al.*, Phys. Plasmas **4**, 1654 (1997).
- ⁴J. S. Sarff, N. E. Lanier, S. C. Prager, and M. R. Stoneking, Phys. Rev. Lett. **78**, 62 (1997).
- ⁵M. N. Rosenbluth, Plasma Phys. Controlled Fusion **41**, A99 (1999).
- ⁶H. P. Furth, J. Killeen, and M. N. Rosenbluth, Phys. Fluids **6**, 459 (1963).
- ⁷J. A. Wesson, Nucl. Fusion **18**, 87 (1978).
- ⁸R. Carrera, R. D. Hazeltine, and M. Kotschenreuther, Phys. Fluids **29**, 899 (1986).
- ⁹P. H. Rutherford, Phys. Fluids **16**, 1903 (1973).
- ¹⁰R. B. White, D. A. Monticello, M. N. Rosenbluth, and B. V. Waddell, Phys. Fluids **20**, 800 (1977).
- ¹¹A. Thyagaraja, Phys. Fluids **24**, 1716 (1981).
- ¹²A. H. Boozer, Phys. Fluids **27**, 2055 (1984).
- ¹³Z. Chang and J. D. Callen, Nucl. Fusion **30**, 219 (1990).
- ¹⁴V. V. Arsenin, L. I. Artemenkov, N. V. Ivanov *et al.*, in *Plasma Physics and Controlled Nuclear Fusion Research 1978*, Proceedings of the 16th International Conference, Innsbruck (International Atomic Energy Agency, Vienna, 1979), Vol. 1, p. 233.
- ¹⁵A. W. Morris, T. C. Hender, J. Hugill *et al.*, Phys. Rev. Lett. **64**, 1254 (1990).
- ¹⁶G. A. Navratil, C. Cates, M. E. Mauel *et al.*, Phys. Plasmas **5**, 1855 (1998).
- ¹⁷E. Lazzaro and M. F. F. Nave, Phys. Fluids **31**, 1623 (1988).
- ¹⁸J. Norris, Plasma Phys. Controlled Fusion **31**, 699 (1989).
- ¹⁹A. Thyagaraja, Plasma Phys. Controlled Fusion **32**, 155 (1990).
- ²⁰M. S. Chu, H. Ikezi, and T. H. Jensen, Phys. Fluids **27**, 472 (1984).
- ²¹The standard large aspect ratio ordering is $R_0/a \gg 1$, where R_0 and a are the major and minor radii of the plasma, respectively.
- ²²The conventional definition of this parameter is $\beta = 2\mu_0 \langle p \rangle / \langle B^2 \rangle$, where $\langle \dots \rangle$ denotes a volume average, p is the plasma pressure, and B is the magnetic field strength.
- ²³W. A. Newcomb, Ann. Phys. (N.Y.) **10**, 232 (1960).
- ²⁴R. Fitzpatrick, Phys. Plasmas **6**, 1168 (1999).
- ²⁵R. Fitzpatrick and F. L. Waelbroeck, Phys. Plasmas **7**, 4983 (2000).